

Spectroscopic investigation of a ‘*Virgin of Sorrows*’ canvas painting: A multi-method approach

M. Ortega-Avilés^{a,1}, P. Vandenabeele^{b,*}, D. Tenorio^a, G. Murillo^a,
M. Jiménez-Reyes^a, N. Gutiérrez^{c,2}

^a ININ, Carretera Federal México-Toluca Km. 36.5, Salazar Edo. Méx., C.P. 52045, Mexico

^b Ghent University (UGent), Department of Analytical Chemistry, Proeftuinstraat 86, B-9000 Ghent, Belgium

^c AHUNAM, Zona Cultural, Delegación Coyoacán, C.P. 04510, Mexico

Received 14 February 2005; received in revised form 13 June 2005; accepted 15 June 2005

Available online 1 August 2005

Abstract

The investigation of unmatched ancient objects is an attentive and arduous activity to conservation scientists. An important aspect of art analysis is the question on sampling and avoiding damage on the artefact during the study. A possible way to maximize the information that is extracted from the historical object is using several sensitive micro-analytical techniques on the same micro samples. As an illustration of this multi-method approach, in this work, a canvas painting ‘*Virgin of Sorrows*’ was studied and its materials were analysed in order to roughly date and to authenticate this object of art. Proton induced X-ray emission (PIXE), neutron activation analysis (NAA), optical microscopy, scanning electron microscopy (SEM), micro-Raman spectroscopy (MRS) and Fourier transform infrared spectroscopy (FT-IR) were used, obtaining successful results. These methods allowed identifying the different inorganic pigments (iron oxide, carbon black, white lead, Prussian blue) as well as indigo. Optical microscopy and SEM revealed the layered structure of the samples, while FT-IR enabled to determine the nature of the varnish used (shellac). By using these complementary techniques, it was possible to identify the materials in the painting, which are indicative for the period of manufacturing the artwork.

© 2005 Elsevier B.V. All rights reserved.

Keywords: Art analysis; Pigments; Oil paintings; Falsification; Proton induced X-ray emission (PIXE); Scanning electron microscopy (SEM); Micro-Raman spectroscopy (MRS); Neutron activation analysis (NAA); Fourier transform infrared spectroscopy (FT-IR)

1. Introduction

Since ancient times, men have collected a large amount of religious art objects. Art production has propitiated a rise and speculation in art prices and together with this, transgressions occur such as theft, falsification and illegal art trade. Mexico is not an exception and thus, it is not surprising to find falsifications of paintings from national artists like,

among others, *José María Velasco* (1840–1912), *Frida Khalo* (1907–1954), *Diego Rivera* (1886–1957) and *José Clemente Orozco* (1883–1949). Colonial paintings and religious motifs have been falsified or copied as well [1].

This work handles on the examination of forgeries in Mexican oil paintings. In Mexico, little historical information is available on the techniques and materials that were used by Mexican artists during the Colonial period (1535–1810 A.D.). Here, the first effort in the country is presented to perform this kind of study, using as much as possible both historical and technical data. An oil painting, representing the ‘*Virgin of Sorrows*’ was studied in this work. It was acquired by a private collector as ‘an ancient painting’, without documentation on its provenance, artist signature or elaboration date. The aim of this study was to date and authenticate

* Corresponding author. Tel.: +32 92646623; fax: +32 92646699.

E-mail addresses: mayahuel@avantel.net (M. Ortega-Avilés), peter.vandenabeele@UGent.be (P. Vandenabeele), nicogz@servidor.unam.mx (N. Gutiérrez).

¹ Tel.: +52 5553297200x3262.

² Tel.: +52 5556226986x2027.

the work. Traditionally, these investigations include image description, investigation of the underdrawing, iconographic analysis, examination of the general condition of conservation and a study of the canvas structure. In this case, all these examinations were performed by a team of art-historians and conservation specialists, who found that the painting was elaborated during the last half of the 18th Century, or the first third of the 19th Century (i.e. between ca. 1750 and 1830). In this type of devotion paintings, the Virgin is depicted with either one or seven swords into her hart, which represents her at the cross, suffering for Christ's sacrifice. The worship of the 'Virgin of Sorrows' appeared in New Spain since the 16th Century and became popular during the 17th and 18th Century, staying popular during almost the whole 19th Century.

In order to be able to identify forgeries as such, several valuable tools are at the investigator's disposal. Obviously, the study of art history and of the cultural heritage helps to solve falsification crimes [2]. Traditionally, dating and the determination of the provenance and the authenticity of artworks have mainly been carried out by art-historians and restorers. In the case of canvas paintings, they focus their interest on aspects such as technique, style, colors, iconography, type of canvas, tensions in the canvas and the state of conservation of the object of art. Most of their investigations are done by the naked eye and by microscopic analysis. Together with the information that is obtained by these methods, consistent evidence of the art materials obtained by means of analytical investigations may help answering specific questions of the art-historians and specialists [3]. In Mexico, during the last years, there is a growing interest for the scientific analysis of antique objects of art. However, an important drawback for the wide application of spectroscopic methods of investigation of antiquities is the fear that the precious artefact might be damaged during analysis. There are discussions going on whether or not it is allowed to sample the artefact for analysis. In any case, if sampling is required or not, the scientist always has to balance the possible risks of damage against the profits that are obtained from the investigation. For each examination, although it is impossible to express this in a numeric format, the risk-of-damage/information ratio should be considered and optimized as much as possible. One way to rise this ratio is done by increasing the amount of information that is obtained from the micro-samples. This is what makes a multi-method approach so favourable.

Today, several methods of experimental physics and analytical chemistry are applied to the identification of pigments in paintings, painted artefacts and antiquities, among them, neutron activation analysis (NAA)[4,5], X-ray diffraction (XRD) [6,7] and X-ray fluorescence (XRF) [8,9]. Analysis by proton induced X-ray emission (PIXE) [10,11], low vacuum-scanning electron microscopy (LV-SEM) [6,7] and micro-Raman spectroscopy (MRS) [8,9,12,13] have been applied for the analysis of paintings. Pigments [4–6,12], binding media and varnishes [13,14] were identified with different aims: to reconstruct the palette of a particular artist or

to obtain historical information on the relationship between populations, trade and migration of cultural groups. Other reasons are to understand the mineralogical background, to provide knowledge on technological evolution, the study of degradation processes of pigments and binding media to help in the preservation and restoration of the objects and to check the authenticity or provenance [1,2,6,8,9,11]. All these studies are based on the analysis of artists' materials, pictorial techniques, manufacture process, etc. During history, painting techniques were conditioned by the size, quality, shape, availability and commercialisation of the painting materials [15–17].

2. Experimental

2.1. Samples

Some investigations could be performed directly on the painting. The areas that have been examined are marked in Fig. 1. In order to be able to perform other investigations as well, sampling of the painting was necessary.

For reasons of comparison, as far as possible, the same positions were sampled, taking advantage of painting's fissures; if not similar shaded areas were chosen (Fig. 1). Samples were labelled Blue-1, Blue-2, Red-3, Red-M4, White-5 and Black-6. They were obtained from the painting by carefully scraping minute portions of the surface from the six col-



Fig. 1. Sampling positions on the 'Virgin of Sorrows' painting. Samples are labelled: (1) Blue-1, medium blue; (2) Blue-2, light blue; (3) Red-3, left hand; (4) Red-M4, left wrist; (5) White-5, veil; and (6) Black-6, bottom of tunic right side.

ored regions (less than $80\ \mu\text{m} \times 50\ \mu\text{m}$ diameter) with a clean and dry sharp scalpel using a $5\times$ magnification for proper observation of the artefact. Samples were not embedded to avoid any contamination and to allow their investigation with multiple analytical techniques. Moreover, samples of canvas fibre (ca. 1 mm) and of the varnish layer were obtained as well.

2.2. Proton induced X-ray emission

PIXE was carried out by using an external beam facility [18]. A tandem Van der Graaf accelerator (High Voltage Inc.) was used with a 2 mm diameter beam spot and an incident angle of 90° in reference to the surface of the painting. A thin aluminium foil (ca. $16\ \mu\text{m}$) was used as window to lead the proton beam spot on the canvas, positioned about 1 cm from the window. The collimator was connected to a current integrator, used as monitor to normalize the proton flux. A proton current of 50 nA was used; the average proton energy was 2.5 MeV. The LN-cooled Si(Li) detector (active area of $10\ \text{mm}^2$ and resolution of ca. 200 eV at 6.4 keV) was located at 4.5 cm from the target, positioned at 52.5° in respect to the sample. The measured intensity flux was kept below 1000 counts/s in order to reduce the spurious pulses and avoid introducing false information of the atomic composition. X-ray spectra were recorded and processed by means of GUPIX software [19]. Calculation of the proton beam penetration depth was performed by means of the SRIM-2003 computer algorithm [20].

2.3. Neutron activation analysis

The possible presence of cinnabar (HgS) was investigated in the samples Red-3 and Red-M4, which were analysed by means of instrumental neutron activation analysis. The samples were irradiated during 15 s with a thermal neutron flux of ca. $1 \times 10^{13}\ \text{cm}^{-2}\ \text{s}^{-1}$ by using the TRIGA MARK III nuclear reactor (ININ, Mexico). After 5 min of decay, the gamma radiation was detected by using a GeH detector.

2.4. Optical microscopy

The layered structure of all the samples was investigated by using a stereoscopic microscope (Karl Zeiss, Axiotech) with a coupled MC80 DX camera. Special regions of interest could be investigated in bright field and dark field mode, by using appropriate filters and magnifications from $10\times$ to $100\times$.

2.5. Low vacuum-scanning electron microscopy

A JEOL JSM-5900LV microscope (resolution of 4 nm) fitted to an energy depressive X-ray microprobe (EDX) was used for micro microscopic and elemental characterization of the paint layers and canvas, upon system calibration. The samples were deposited on a brass cylinder, by sticking them

with carbon tape, trying to reach as nearly as possible a horizontal surface on the transversal section as observed with optical microscopy. By doing so, good electron and X-ray signals could be obtained. Images were obtained by mean of secondary electron signals as secondary electron images (SEI) with energies from 10 to 20 keV, vacuum pressure from 12 to 17 psi and working distance from 7 to 10 mm.

2.6. Micro-Raman spectroscopy

Micro-Raman spectroscopy was performed on the samples by using a Renishaw System-1000 spectrometer that was equipped with a 50 mW, 785 nm diode laser. Laser power on the sample could be reduced by using a set of neutral density filters, to avoid any thermal damage. Typically, laser power was set below 0.5 mW at the sample. By using the $80\times$ objective lens, a laser spotsize of ca. $1\ \mu\text{m}$ could be obtained. After dispersion on a $1200\ \text{lines}\ \text{mm}^{-1}$ dispersion grating, the Raman signal was detected by a Peltier-cooled CCD-detector, allowing to record spectra with a spectral resolution of $1\ \text{cm}^{-1}$. More details on experimental set-up are given elsewhere [9,13]. Raman spectra were recorded between the laser line and $2200\ \text{cm}^{-1}$, with typical accumulation times of 300 s. Pigment grains were selected at random as well as by visual inspection to check for obvious abnormalities. Typically, per sample 10–15 spectra were recorded.

2.7. Fourier transform infrared spectroscopy

Fourier transform infrared spectroscopy was performed on the varnish sample in order to obtain its absorption spectrum and to make a comparative study with a modern varnish. The analysis was performed with a Nicolet MAGNA 550 spectrometer to examine the region from 400 to $4000\ \text{cm}^{-1}$ with 40 scans at a resolution of $4\ \text{cm}^{-1}$ in transmission mode. About 1 mg of the solid varnish was grounded in a small agate mortar with 80–100 times its bulk of pure potassium bromide (Merck) and the mixture was moulded to obtain a flat pellet of 7 mm diameter.

3. Results and discussion

3.1. Elemental analysis: PIXE and NAA

Several colored areas have been examined by using PIXE (Fig. 2). The colors of the painting under study are red, flesh tones, blue, white and black and the result of the elemental analysis is given in Table 1. Most of the samples show high amounts of Pb, an element that is highly indicative for the presence of white lead ($2\text{PbCO}_3 \cdot \text{Pb}(\text{OH})_2$). This pigment might be used as whitener or as siccativ. When comparing the darker tones with the brighter ones (i.e. red with flesh and medium blue with light blue), it is seen that the latter are richer in Pb content. In the black area of the tunic, only a very small amount of Pb (white lead) is detected, which is

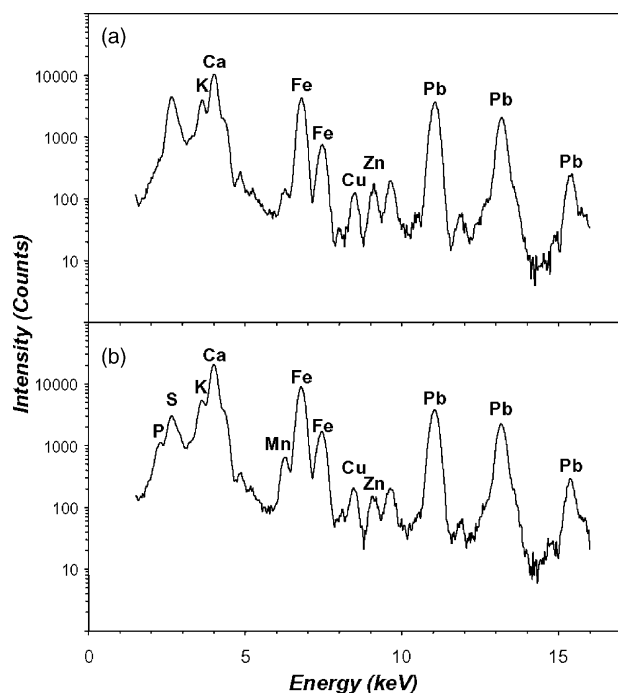


Fig. 2. PIXE spectra: (a) blue light region; (b) black region.

consistent with the idea of using white lead as a whitener. The relatively high content of Pb in the PIXE results from the black eyebrow, may originate from the composition of the underlying layer, as the eyebrow is painted over the flesh tones of the face, this is reflected in the elemental composition.

All the PIXE results show a significant amount of Ca, which may originate from CaCO_3 or gypsum ($\text{CaSO}_4 \cdot \text{H}_2\text{O}$),

evidently used as an addition to the white lead in the preparation layer on the canvas. The amounts of sulphur seem to suggest the presence of the latter pigment, although sulphur might even so well originate from the binding medium that is applied. The black area contains high amounts of Ca, eventually an admixture of CaCO_3 , used as a loading [15]; the black pigment is probably carbon black, which is not detected by PIXE.

The analysis of the red sleeve shows a significant amount of Fe, a result that indicates the presence of iron oxide, such as hematite (Fe_2O_3); hematite can be applied as a pure pigment, but it is even so well the main component of red ochre. In the flesh tone areas, no significant amount of Fe was present; the pigment might be diluted with white lead as well as an organic pigment might be present. Due to peak overlap of Pb $L\alpha$ (10.55 keV) with Hg $L\alpha$ (9.9 keV), PIXE analysis could not exclude the presence of natural or synthetic vermilion (HgS). In order to reveal the eventual presence of Hg, instrumental neutron activation analysis was performed on a red sample from the left sleeve (Red-M4) and on a flesh tone sample from the left hand. Gamma spectrometry of the activated samples did not reveal the presence of any mercury isotope; therefore, vermilion could be discarded as a component of the red samples.

Significant amounts of Fe in the blue areas seem to indicate the use of Prussian blue ($\text{Fe}_4[\text{Fe}(\text{CN})_6]_3$), a pigment that was synthesized for the first time by Diesbach in Berlin in 1704 [21]. Next to this, the high Fe content in many areas can be attributed to the red bole which has been applied over different thicknesses probably as under-drawing. This is as well observed in the white region. The high Fe content in the blue area originates from a contribution of blue and the red underdrawing. The Fe signal of the red (flesh) samples is suppressed by a thin layer of whitelead on top.

Table 1

Chemical composition (percentage of elements) of the samples by PIXE (+ indicates an amount below the quantification limit; n.d. indicates a value below the limit of detection)

Elements (%)	Red left sleeve	Red finger right hand	Red right hand	Red fronthead	Medium blue right sholder	Light blue left sleeve of tunic	White sword	Black left eyebrow	Black front of canvas (tunic)	Black background of canvas
Si	+	+	+	+	+	+	+	+	+	+
P	+	+	+	+	+	+	+	+	+	+
S	5.2 ± 0.7	5.3 ± 0.5	3.0 ± 0.6	6.0 ± 0.5	3.1 ± 0.9	3.2 ± 0.9	3.7 ± 0.7	4.9 ± 0.7	5 ± 1	4 ± 2
K	3.8 ± 0.7	1 ± 2	1 ± 3	1 ± 2	1 ± 2	1 ± 3	2 ± 1	2 ± 1	11 ± 1	10.4 ± 0.9
Ca	4.3 ± 0.6	5.0 ± 0.3	2.6 ± 0.4	4.6 ± 0.3	3.8 ± 0.5	2.3 ± 0.7	3.1 ± 0.6	4.2 ± 0.5	36.5 ± 0.2	31.4 ± 0.3
Ti	+	+	+	+	+	+	+	+	+	+
Mn	+	+	+	+	+	+	+	+	+	+
Fe	2.5 ± 0.6	+	+	+	4.1 ± 0.6	3.0 ± 0.8	4.1 ± 0.5	1.1 ± 0.9	+	3 ± 1
Co	+	n.d.	n.d.	n.d.	+	n.d.	+	n.d.	n.d.	n.d.
Cu	+	+	+	+	+	+	+	+	+	+
Zn	+	+	+	+	+	+	+	+	+	+
Ru	+	+	+	+	+	+	+	+	+	+
Ce	+	n.d.	+	n.d.	+	n.d.	n.d.	+	+	n.d.
Hg	+	+	+	+	+	+	+	+	+	+
Pb	56.1 ± 0.6	65.1 ± 0.5	78.7 ± 0.4	65.5 ± 0.4	68.3 ± 0.6	75.7 ± 0.6	68.2 ± 0.5	64.2 ± 0.5	3 ± 4	9 ± 2

Detection limit: 1–2 ppm after 300 s of analysis; n.d. = not detected; (+) = possible presence.

3.2. Microscopic analysis: optical microscopy and LV-SEM

The samples of the painting have been examined with optical microscopy (Fig. 3a) and low vacuum-scanning electron microscopy (Fig. 3b and c, Fig. 4). An overview of the layered structure is given in Table 2. All the samples consist of up to six different layers, which reveal part of the painting technique that has been used. Apparently, before painting, the canvas has been prepared with a white ground layer. This is

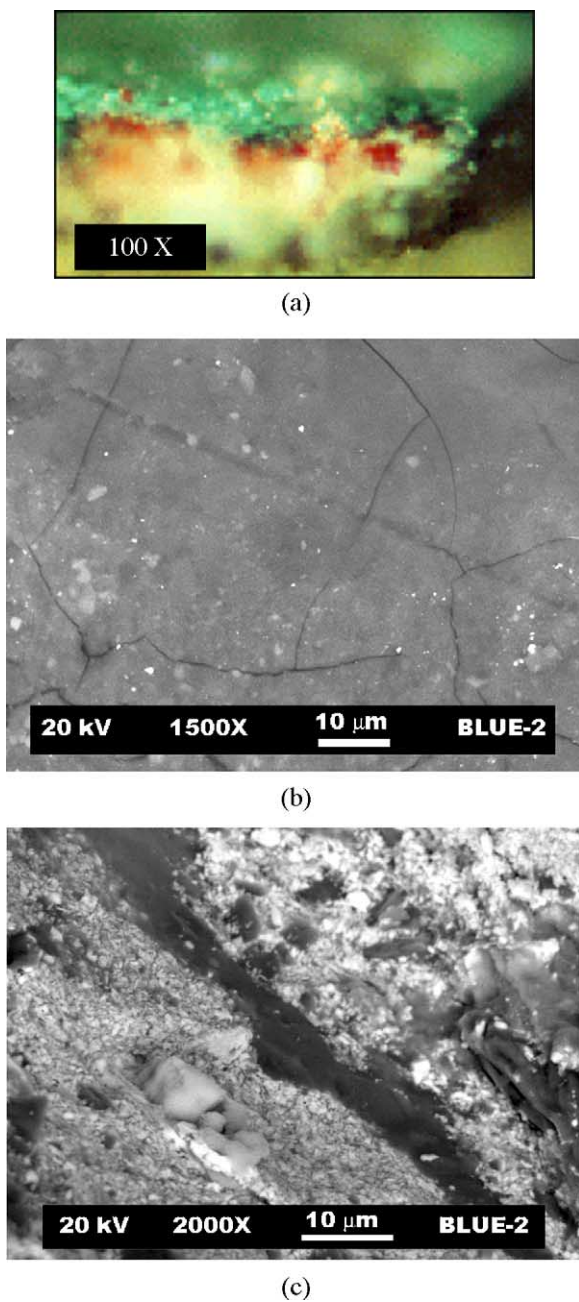


Fig. 3. Blue-2 sample: (a) color picture in cross section 100 \times ; (b) protection varnish layer 1500 \times , BEI, 17 psi; (c) cross section micrograph 2000 \times , BEI, 17 psi.

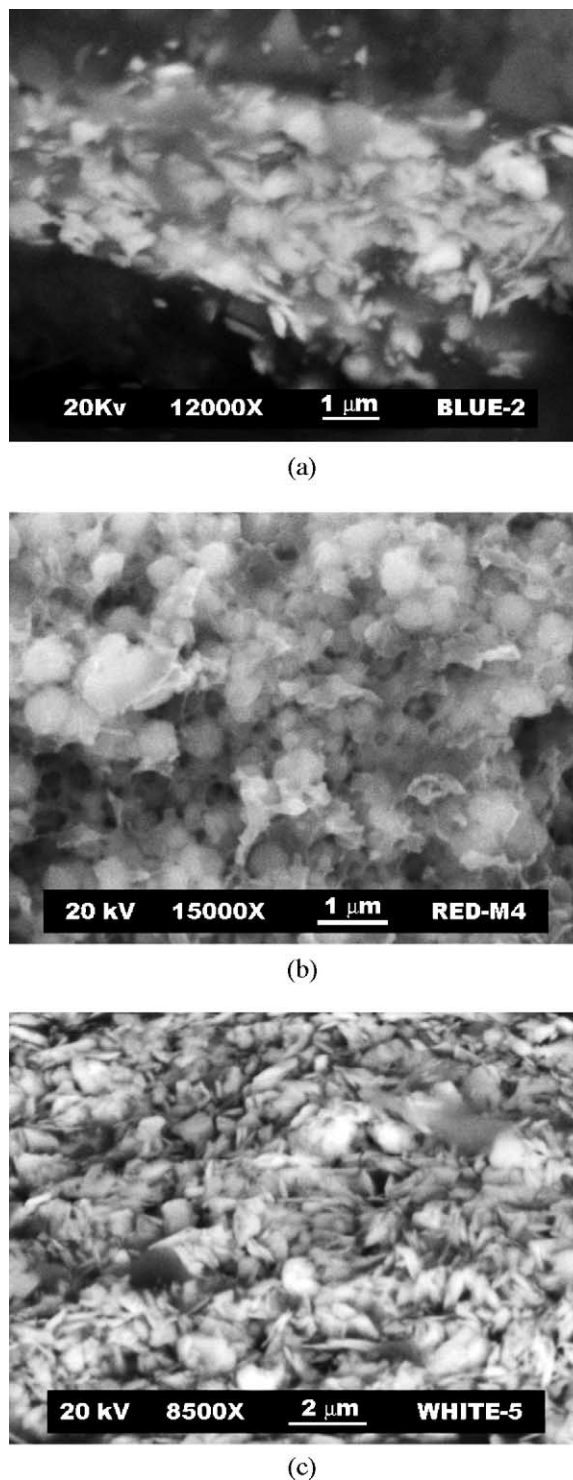


Fig. 4. LV-SEM micrographs: (a) Blue-2, BEI, 17 psi; (b) Red-M4 after varnish dissolution, BEI, 17 psi; (c) White-5, BEI, 12 psi.

consistent with the suggestion of a calcite-containing preparation layer, from the PIXE analysis. In almost all the samples, a red paint layer is found, covered with a thin varnish layer. This finding seems to suggest that the artist has painted the contours of the figure by using a red bole, before overpainting it with blue, black and white paint layers.

Table 2
Thickness of the different layers in the samples, by microscopic analysis (n.d. = not detected)

Stratigraphic layers thickness (μm)	Samples					
	Blue-1 (medium blue)	Blue-2 (light blue)	Red-3	Red-M4	White-5	Black-6
Varnish	20	10–20	15	15	10–20	10
Black	10					25–30
White			10	10	20–30	
Blue	10	15–20				
Varnish	n. d.	3–5	10	10	5	
Red	25–30	10	20–25	10–20	20–30	
White	n. d.	n. d.	n. d.	n. d.	n. d.	~80

By mean of LV-SEM, superficial inspection was performed and we could detect countless crackles were observed in average ca. $1 \mu\text{m}$ wide; superficial damage could occur due to natural varnish ageing and degradation in all the samples (Fig. 3b). Element analysis by EDX resulted in 82.57 at.% of C and 17.43 at.% of O for the sample Blue-2. This, along with the absence of high concentrations of Cu or Co, might indicate the presence of an organic blue pigment. The cross section micrograph of this sample (Fig. 3c) shows three layers: red, varnish and blue. In the red and blue layers, it was possible to observe heterogeneity in particle size, large Ca-rich particles of $10 \mu\text{m}$ immersed in very small Fe-rich particles. Varnish layer thickness changed, depending on the sample area between ca. 5 and $10 \mu\text{m}$. The blue layer (Fig. 4a) contains particles with different contrast: dark amorphous varnish regions, bright particles rich in Pb and small particles of intermediate contrast containing considerable amounts of Fe, C, N, Ca, S and Na. In the case of the sample Red-M4, EDX suggested that the red paint was Fe-rich, probably from iron ores. It was necessary to remove the varnish in which red particles were immersed in order to observe their morphology, by dissolving the varnish in ethanol the typical morphology of iron oxide particles of $0.5\text{--}1 \mu\text{m}$ could be observed (Fig. 4b). Many flakes of about $2 \mu\text{m}$ of length were observed for the area White-5 (Fig. 4c). Pb, C, O, Mg, Al and Ca were identified by EDX; the layer was Pb-rich with some

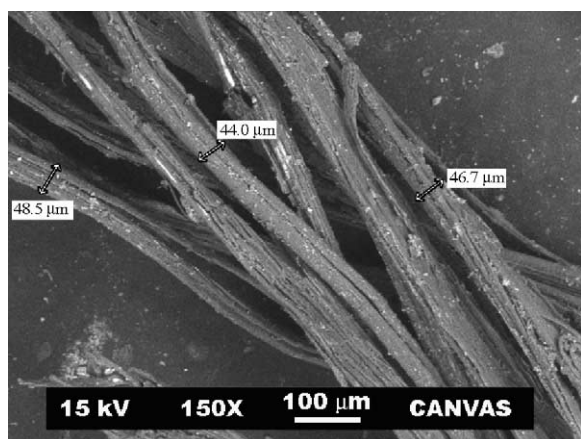


Fig. 5. Canvas morphology, BEI, 12 psi.

particles containing Ca, probably an admixture of lead white on calcium carbonates, which was used as preparation layer. The black pigment contained carbon.

The Canvas was most likely made of linen, considering its morphology as observed by LV-SEM. These fibers have a diameter ranging from 74.4 to $48.5 \mu\text{m}$ (Fig. 5). The EDX spectrum showed mainly C (69.26 at.%) and O (29.35 at.%) and Na, Mg, Al, Si, S, Cl, K and Ca in minor quantities.

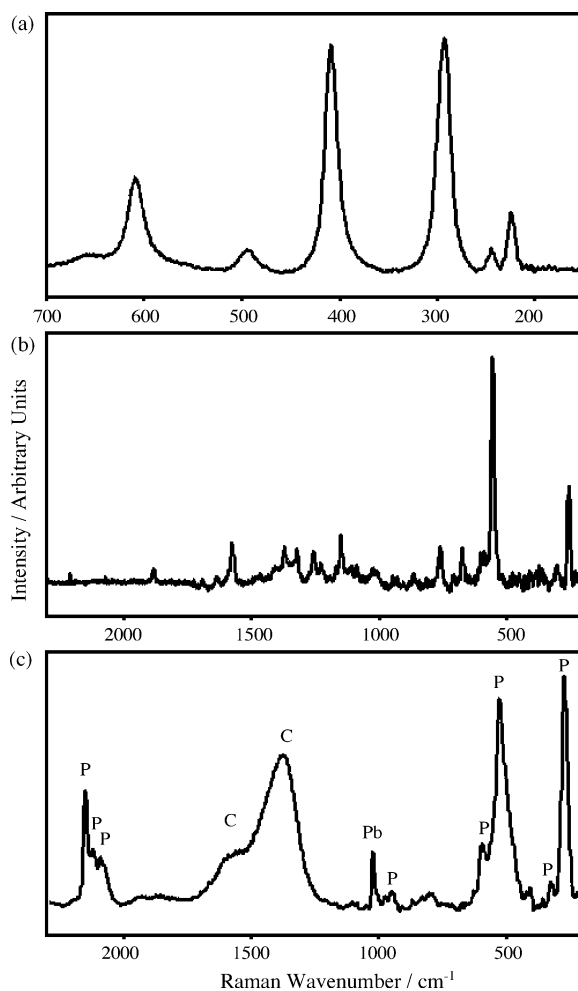


Fig. 6. Raman spectra from: (a) sample Red-M4, revealing the spectrum of hematite; (b) sample Blue-1, showing the spectrum of indigo; and (c) sample Blue-2 (P = Prussian blue, C = carbon black and Pb = white lead).

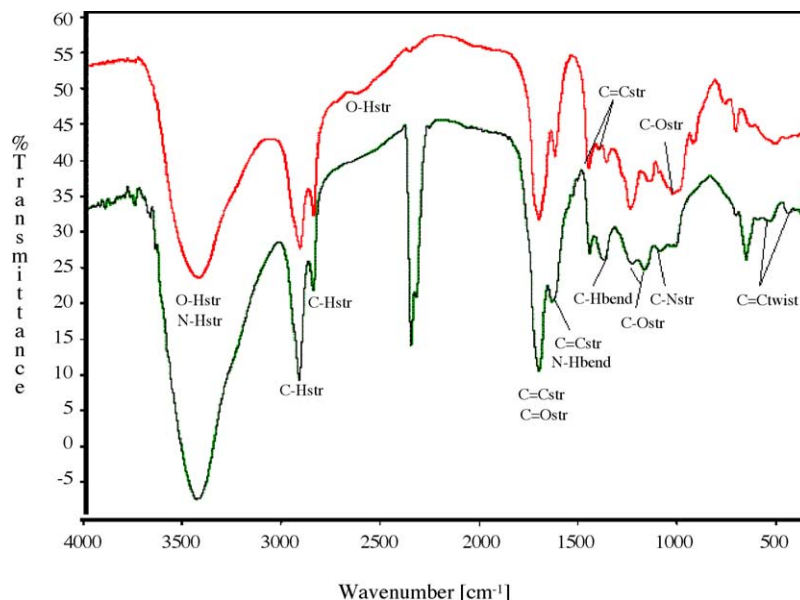


Fig. 7. FT-IR spectra: (Top) modern commercial shellac; (Bottom) varnish on the canvas painting.

3.3. Molecular spectroscopic analysis: MRS and FT-IR

Micro-Raman spectra were recorded of some of the samples, in order to reveal the molecular composition of the paint layers. Different pigments could be identified. In the red samples, hematite (Fe_2O_3 , Fig. 6a) was identified, which is in agreement with the results from PIXE and LV-SEM. The white areas contained calcite (CaCO_3), which is easily identified from its main Raman band positions (1086 and

712 cm^{-1}) and some traces of white lead as well as gypsum. The blue regions contained definite amounts of Prussian blue ($\text{Fe}_4[\text{Fe}(\text{CN})_6]_3$, Fig. 6c), which was as well suggested by the results of the PIXE analysis. Especially, the presence of the $\nu(\text{C}\equiv\text{N})$ stretching vibration, reflected in a Raman band around ca. 2200 cm^{-1} , is highly specific for this pigment. Next to the presence of this inorganic pigment, Raman spectroscopy is also able to identify organic colorants. In the same blue samples, indigotin could be observed (Fig. 6b)

Table 3
Band assignments for the FT-IR spectra (s = strong, m = medium intensity and w = weak)

Varnish on the canvas painting (wavenumber (cm^{-1}))	Modern commercial shellac (wavenumber (cm^{-1}))	Intensity	Vibrational modes
3448	3434	s	O–H str alcohol, N–H str
2927	2923	s	C–H str
2857	2854	m	C–H str methyl
	2642	w	O–H str carboxylic acids
2363	2367	s	
2338		s	
1718	1717	s	C=C str
1655	1636	m	C=O str carboxylic acids, ketones N–H bend amines C=C str aromatic rings
1459	1466	m	C=C str aromatic rings
	1415	m	C=C str aromatic rings
1384	1375	w	C–H bend ring
1257	1254	m	C–O str carboxylic acids
1183	1163	w	C–O str carboxylic acids
1103		m	C–N str amines
1023	1040	m	C–O str carboxylic acids
	942	w	
	775	w	
723	723	w	
672	650	m	
556	521	w	C=C twist
470	467	w	C=C twist

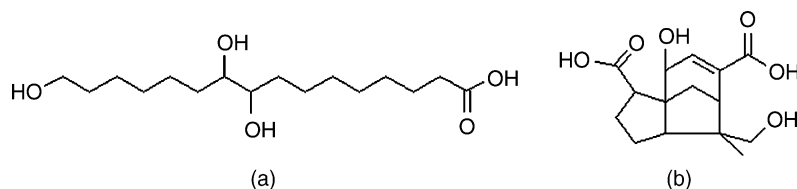


Fig. 8. Structures of (a) aleuritic acid and (b) shelloic acid, the two main compounds of shellac.

along with the Prussian blue, confirming the suggestion of an organic pigment, as made by the LV-SEM and EDX measurements. To obtain a darker shade of blue, in some regions carbon black was admixed. This was also the black pigment that was identified in the black areas. In these samples, by using micro-Raman spectroscopy, it was not possible to identify the binding medium.

In order to identify the varnish that was used on the painting, IR spectra of modern commercial shellac (Casa Serra (Mex)) and of the varnish on the canvas painting were compared (Fig. 7 and Table 3). The absorption bands of the original varnish spectrum show a little redshift in respect to the modern shellac sample, but the correspondence is striking; in the fingerprint region, characteristic bands are found between 700 and 950 cm^{-1} , namely at 945, 930 and 724 cm^{-1} . Other characteristic bands are found around 1735 and 1715 cm^{-1} , which can be attributed to $\nu(\text{C}=\text{O})$ stretching vibrations. The intense absorption band at ca. 2300 cm^{-1} in the varnish spectrum can be assigned to the $\text{C}\equiv\text{N}$ stretching vibration, originating from a minute trace of Prussian blue. Our spectrum of modern shellac is in good agreement with the spectrum of natural shellac, as reported by Derrick et al. [22,23].

Shellac or gum-lac is a natural polymer, the flaked and purified form of a resinous substance (lac) secreted by *Lacifer lacca* [21,24]. The scraped lac, known as crude lac or sicklac, consists of resin, lac dye, the encrusted insects and twigs. After crushing, washing and drying seedlac is formed, which can be converted by mild hydrolysis into shellac. Shellac mainly consists of esters of aleuritic acid (46%), shelloic acid (27%) (Fig. 8) or esters of aleuritic acid and jalaric acid.

4. Conclusions

In this paper, it was demonstrated that a combined method approach, performed directly on the artwork and on small samples, is able to identify the materials that were used to manufacture an artefact. The consequences of these findings, in relation to dating and authenticating the artefact, are consistent with the art historical observations. We can conclude that this 'Virgin of Sorrows' canvas painting was elaborated during last middle of the 18th Century or the early third of the 19th Century.

In a broader context, this paper proves that the combination of elemental analysis (PIXE, NAA) with microscopic techniques (light microscopy and SEM) and vibrational spec-

troscopic techniques (FT-IR and Raman) form a good combination to tackle problems in the field of art analysis based on a complete characterization of organic and inorganic components.

Each of the applied techniques provides different information on the samples. PIXE and NAA were used to determine the element composition of the pigments: both techniques are able to detect elements with $Z > 13$ and assisted to prove the absence of Hg (Vermilion, HgS) in the red pigments. Microscopic techniques provided information regarding the stratigraphic composition and allowed to distinguish between the composition of the surface layer and of the different layers underneath. Additionally, EDX analysis confirmed the elemental composition of the pigment grains as previously determined by PIXE and NAA. Spectroscopic analysis by means of micro-Raman spectroscopy was useful to confirm the presence of some pigments like Prussian blue, hematite and white lead, but this technique allowed as well to reveal the presence of indigo in blue samples. FTIR is a good option to identify organic compounds, such as the varnish layer of this artwork.

Acknowledgements

This research was conducted in the National Institute of Nuclear Research in collaboration with the Department of Analytical Chemistry of Ghent University. We thank Mr. Pedro Meshia and Carlos Flores (IFUNAM-UNAM) for their excellent cooperation. The team at Ghent University acknowledges the Fund for Scientific Research-Flanders (F.W.O.-Vlaanderen) and the research council of Ghent University (BOF) for their financial support. P.V. is especially grateful to the Fund for Scientific Research-Flanders (F.W.O.-Vlaanderen) for his postdoctoral fellowship.

References

- [1] Z.N. Gutiérrez, Técnicas Físicoquímicas e Instrumentales Utilizadas en la Detección de Falsificaciones de Obra Gráfica: Alcances y Limitaciones, Master Thesis, México, 2001.
- [2] O. Debroise, Fascinación de lo Falso, La Falsificación y sus Espejos. Artes de México, 28, México, 1995.
- [3] M.A. Cabrera, Los Métodos de Análisis Físico-Químicos y la Historia del Arte, Granada (1994).
- [4] M. Peisach, C.A. Pineda, L. Jacobson, J. Radioanal. Nuc. Chem. 151 (1) (1991) 221–227.

- [5] D. Tenorio, M. Jiménez-Reyes, A. Cabral-Prieto, M.G. Siles-Dotor, H. Flores-Ramírez, J.L. Galván-Madrid, *Hyperfine Interact.* 128 (2000) 381–396.
- [6] M. Ortega, J.A. Ascencio, C.M. San-Germán, M.E. Fernández, M. José-Yacamán, *J. Mater. Sci.* 36 (3) (2001) 751–756.
- [7] M. Ortega-Avilés, C.M. San-Germán, D. Mendoza-Anaya, D. Morales, M. José-Yacamán, *J. Mater. Sci.* 36 (9) (2001) 2227–2236.
- [8] P. Vandenabeele, A. Von Bohlen, L. Monees, R. Klockenkämper, F. Joukes, G. Ddewispelaere, *Anal. Lett.* 33 (15) (2000) 3315–3332.
- [9] B. Wehling, P. Vandenabeele, L. Moens, R. Klockenkämper, A. Von Bohlen, G. Van Hooydonk, M. De Rue, *Microchim. Acta* 130 (1999) 253–260.
- [10] T. Tuurnala, A. Hautajarvi, K. Harva, *Stud. Conserv.* 30 (1985) 86–92.
- [11] M.I. Dinator, J.R. Morales, *J. Radioanal. Nuc. Chem.* 140 (1) (1990) 133–139.
- [12] P. Vandenabeele, L. Moens, H.G.M. Edwards, R. Dams, *J. Raman Spectrosc.* 31 (2000) 509–517.
- [13] P. Vandenabeele, B. Wehling, L. Moens, H. Edwards, M. De Reu, G. Van Hooydonk, *Anal. Chim. Acta* 407 (2000) 261–274.
- [14] Glosario de Adhesivos y Consolidantes, Dirección de Restauración del Patrimonio Cultural, INAH, México (1989) 9–11.
- [15] A. Carrillo y Gariel, *Técnica de la Pintura de la Nueva España*, 39, Imprenta Univesitaria, México, 1946, pp. 39–83.
- [16] M. Bazzi, *Enciclopedia de las Técnicas Pictóricas*, Noguer, Barcelona, 1965.
- [17] M. Doerner, *Los Materiales de la Pintura y su Empleo en el Arte*, Reverté, 1965.
- [18] J.A. Maxwell, L. Campbell, W.J. Teesdale, The guelph PIXE software package, *Nucl. Instrum. Methods Phys. Res.* B43 (1989) 218–230.
- [19] M. Fernández, R. Policroniades, G. Murillo, E. Moreno, F.I. Jiménez, Technical Report CA 94-04 ININ, México, 1994.
- [20] J.P. Ziegler, L. Haggmark, *Bucl. Inst. Methods* 174 (1980) 257.
- [21] R.J. Gettens, G.L. Stout, *Painting Materials: A Short Encyclopedia*, D. Van Nostrand, New York, 1947.
- [22] M.R. Derrick, D.C. Stulik, J.M. Landry, S.P. Boufard, *J. Am. Inst. Conserv.* 31 (2) (1992) 227–229.
- [23] M.R. Derrick, *J. Am. Inst. Conserv.* 28 (1) (1989) 43–56.
- [24] J.S. Mills, R. White, *The Organic Chemistry of Museum Objects*, second ed., Butterworth and Heinemann, Oxford (UK), 2003, pp. 115–118.